Food Hydrocolloids 151 (2024) 109814

Contents lists available at ScienceDirect

Food Hydrocolloids

journal homepage: www.elsevier.com/locate/foodhyd

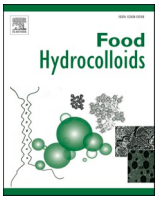

Pectin and pectin/chitosan hydrogel beads as coffee essential oils carrier systems

Luis Henrique Reichembach [a], Carmen Lúcia de Oliveira Petkowicz [a], Pedro Guerrero [b,c], Koro de la Caba [b,c,*]

[a] Department of Biochemistry and Molecular Biology, Federal University of Parana, PO Box 19046, 81531-980, Curitiba, Parana, Brazil
[b] BIOMAT Research Group, University of the Basque Country (UPV/EHU), Escuela de Ingeniería de Gipuzkoa, Plaza de Europa 1, 20018, Donostia-San Sebastián, Spain
[c] BCMaterials, Basque Center for Materials, Applications and Nanostructures, UPV/EHU Science Park, 48940, Leioa, Spain

ARTICLE INFO

Keywords:
Pectin
Chitosan
Essential oils
Controlled release

ABSTRACT

Two pectin fractions extracted from coffee pulp, one high-methoxylated (*Coffea arabica* pectin, CAP) and other low-methoxylated (chelating agent-soluble pectic fraction, CSP), were used for the development of hydrogel beads loaded with coffee roasted and green essential oils (EOs). The aim of the study was to compare the two types of pectin, with or without chitosan, on their encapsulation performance for the delivery of EOs. Systems were analyzed regarding their rheological, morphological, physicochemical and mechanical properties. Association with chitosan reinforced the beads, which showed better mechanical properties and resisted to acidic and basic treatments, influenced by EO type. ATR-FTIRspectroscopy and X-ray diffraction were performed to assess structural characteristics and interactions of the different samples. The analyses showed that alkaline treatment caused more structural modifications than the acidic treatment in the polysaccharide matrix. Swelling ability of CAP was higher than that of CSP, and green coffee oil prevented bead degradation by acids. Controlled release was carried out in fatty food simulant, and the formulations containing CAP and chitosan had the highest release values. DPPH radical scavenging activity showed that coffee essential oils can act as antioxidants, with the roasted coffee oil presenting superior antioxidant activity.

1. Introduction

Hydrogel beads are delivery systems that can be prepared from many food-grade hydrocolloids (Zeeb, Saberi, Weiss, & McClements, 2015). They are generally formed by a solution containing a mixture of nutraceuticals and biopolymers followed by a cross-linking that leads to the formation of a hydrogel within the beads. Polysaccharides are widely used for gel formation and the ones that are dietary fibers are not degraded within the upper gastrointestinal tract, being that the release only occurs in the colon (McClements, 2017).

One of the main natural polymers used for gelation and delivering of molecules of interest is pectin (Mishra, Datt, Pal, & Banthia, 2008). Pectins are anionic plant polysaccharides well known for its gelling (Bemiller, 1986; Willats, Knox, & Mikkelsen, 2006) and emulsifying and emulsion-stabilizing properties (Leroux, Langendorff, Schick, Vaishnav, & Mazoyer, 2003; Ngouémazong, Christiaens, Shpigelman, Van Loey, & Hendrickx, 2015). They are traditionally extracted from citrus peel and apple pomace; however, alternative sources have been extensively studied in the last few decades. Coffee pulp is one of these materials, showing an increasing interest due to its abundance, low cost and availability. Structural features of coffee pulp pectins have been previously investigated (Reichembach, Kaminski, Maurer, & Petkowicz, 2024; Reichembach & Petkowicz, 2020).

Pectin alone exhibits limited water barrier properties due to their inherent hydrophilic nature. Improvements in water resistance and mechanical properties of pectin materials can be achieved by combining pectin with other polymers, as for example chitosan. Chitosan has been widely employed as a key macromolecule to reinforce the polymer matrix (Reichembach & Petkowicz, 2021). Chitosan is a cationic polysaccharide widely used in food science. Chitosan matrices can be used to protect encapsulated materials, control release, reduce toxicity, and facilitate targeted delivery after absorption from the gastrointestinal tract. Chitosan's appeal lies in its mucoadhesive ability, permeation-enhancing effects, ease of modification, and cationic

* Corresponding author. BIOMAT Research Group, University of the Basque Country (UPV/EHU), Escuela de Ingeniería de Gipuzkoa, Plaza de Europa 1, 20018, Donostia-San Sebastián, Spain.
E-mail address: koro.delacaba@ehu.es (K. de la Caba).

https://doi.org/10.1016/j.foodhyd.2024.109814
Received 8 November 2023; Received in revised form 22 January 2024; Accepted 24 January 2024
Available online 25 January 2024

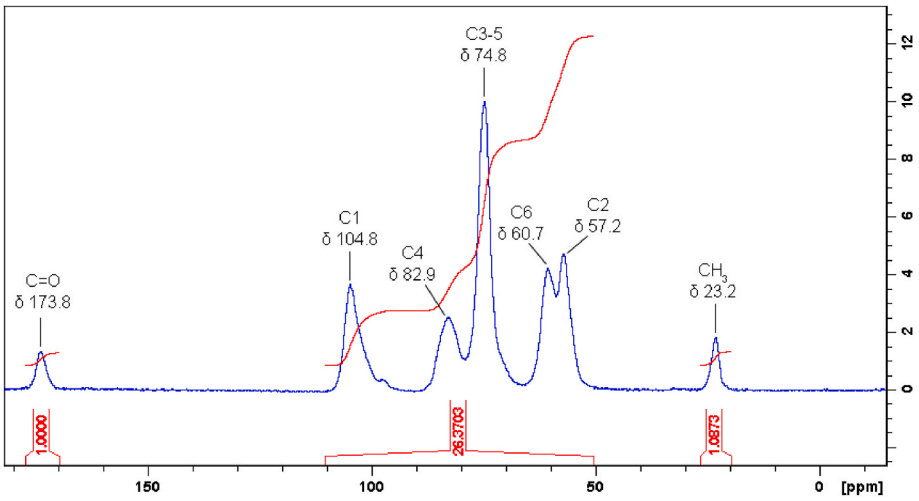

Fig. 1. CP-MAS ^{13}C NMR spectrum of chitosan (CHI) and relative integral of the peaks used for DA estimation.

characteristics (Qu & Luo, 2020).

Among the bioactive compounds used in food systems, EOs are ones that require encapsulation for maintaining stability. EOs are volatile, aromatic liquids with antioxidant and antimicrobial properties, offering a natural alternative for food preservation (Tongnuanchan & Benjakul, 2014). They gain attention as an eco-friendly substitute for chemical preservatives, which often pose environmental and health risks (Maurya, Prasad, Das, & Dwivedy, 2021). The encapsulation of EOs ensures that their functional properties are maintained, the volatility is reduced, and the dispersion across food surfaces is facilitated (Ju et al., 2019). In addition, the encapsulation procedure provides higher stability to the EO compounds through digestion, ensuring its bioactivity in the human organism (Razola-Díaz, Guerra-Hernández, García-Villanova, & Verardo, 2021).

Coffee oil, considered a vegetable or essential oil due to its fatty acids and volatile compounds, is generally recognized as safe (GRAS) and widely used in cosmetics for its emollient, antioxidant, and UV-blocking effects (De Oliveira et al., 2014; FDA, 2023). Comprising mainly triacylglycerols, diterpene alcohols, and sterols, green coffee oil, especially from *Coffea arabica*, is characterized by the presence of diterpenes like cafestol and kahweol, which exhibit anti-inflammatory, anti-angiogenic, anti-tumorigenic, antioxidant, and hepatoprotective properties (Calligaris, Munari, Arrighetti, & Barba, 2009; De Oliveira et al., 2014; Ren, Wang, Xu, & Wang, 2019).

In this work, the potential of a high methoxylated (HM) and a low methoxylated (LM) pectic fraction from coffee pulp for the development of pectin and pectin/chitosan hydrogel beads loaded with green and roasted coffee EOs was evaluated. The novelty of the work lies on the proposal of the use of different pectins extracted from a large produced waste for the release of two different types of coffee EOs, which allows a comparison between pectin or oil type and the performance of hydrogel beads as delivery systems. The study aimed to evaluate the encapsulation performance of two types of pectin, with and without chitosan, in delivering essential oils.

2. Materials and methods

2.1. Materials

The pectins, CAP (79.5 % GalA; degree of methyl-esterification 63.2 %; M_w 3.9 × 10^5 g/mol) and CSP (50.5 % GalA; degree of methyl-esterification 9.0 %; M_w 4.8 × 10^5 g/mol) were isolated from coffee pulp and previously characterized (Reichembach et al., 2024; Reichembach & Petkowicz, 2020). Chitosan (CHI) from shrimp shells (Sigma-Aldrich, Spain), with high molecular weight (M_w 3.75 × 10^5 g/mol), was used. Green and roasted coffee EOs were purchased from a natural products store (Terra Flor, Brazil). The other reagents were of analytical grade.

2.2. Preparation of pectin and pectin/chitosan beads loaded with coffee EOs

Coffee pulp pectin solutions were prepared in Milli-Q water at a concentration of 5 % (w/v) by mechanical stirring. After complete dissolution of 2.5 g pectin, 500 μL of roasted or green coffee EOs (20 % (v/w) in relation to pectin) were added to the solution and mixed at 8000 rpm for 5 min for the formation of an emulsion (Ultraturrax UT25, IKA, Germany). Pectin/chitosan solutions were produced in Milli-Q water at a concentration of 1 % (w/v). Firstly, 0.5 g pectin was dissolved in 25 mL Milli-Q water and then 100 μL (20 % (v/w) in relation to pectin) of coffee EO was added and mixed at 8000 rpm for 5 min for emulsification. Chitosan (0.5 g) was dispersed in water (21 mL) for 10 min and then 1 M acetic acid (4 mL) was added. The chitosan solution was mixed at 8000 rpm for 10 min (Ultraturrax UT25, IKA, Germany) and the previously prepared pectin/EO emulsion was added and stirred at 8000 rpm for other 10 min. Controls were prepared without the addition of EOs.

Beads were prepared by dripping the polymer dispersions in proper solution using a 2 mL syringe. For pectin bead formation, a 1 % (w/v) $CaCl_2$ solution was used, while for pectin/chitosan beads, a solution containing 4 % (w/v) sodium triphosphate penta-basic (TPP) and 5 % (w/v) NaOH solution was employed. The beads were stirred for 30 min at 80 rpm to promote crosslinking and then washed for 30 min over running tap water. The beads were frozen for conservation and thawed at 4 °C the day prior to the analyses.

2.3. Degree of N-acetylation (DA)

The DA of chitosan was determined by solid-state Cross-Polarization Magic Angle Spinning ^{13}C Nuclear Magnetic Resonance (CP/MAS-^{13}C NMR) using a Bruker 400 Avance III 400 WB spectrometer 9.40 T with a resonance frequency of 400 MHz. Glycine was used as external reference (δ of carbonyl peak at 176 ppm). The calculation of DA was done by the ratio of the average of the relative integral values of the carbonyl and methyl groups to the average of the integral values of the backbone carbon atoms (Heux, Brugnerotto, Desbrières, Versali, & Rinaudo, 2000), as shown in the following equation:

$$DA\ (\%) = \left(\frac{I_{CH3}}{\frac{I_1+I_2+I_3+I_4+I_5+I_6}{6}} + \frac{I_{C=O}}{\frac{I_1+I_2+I_3+I_4+I_5+I_6}{6}} \right) \times \frac{1}{2} \times 100$$

where $I_{1\text{-}6}$ is the integral respective to the signals of the ring carbons ($C_{1\text{-}}$

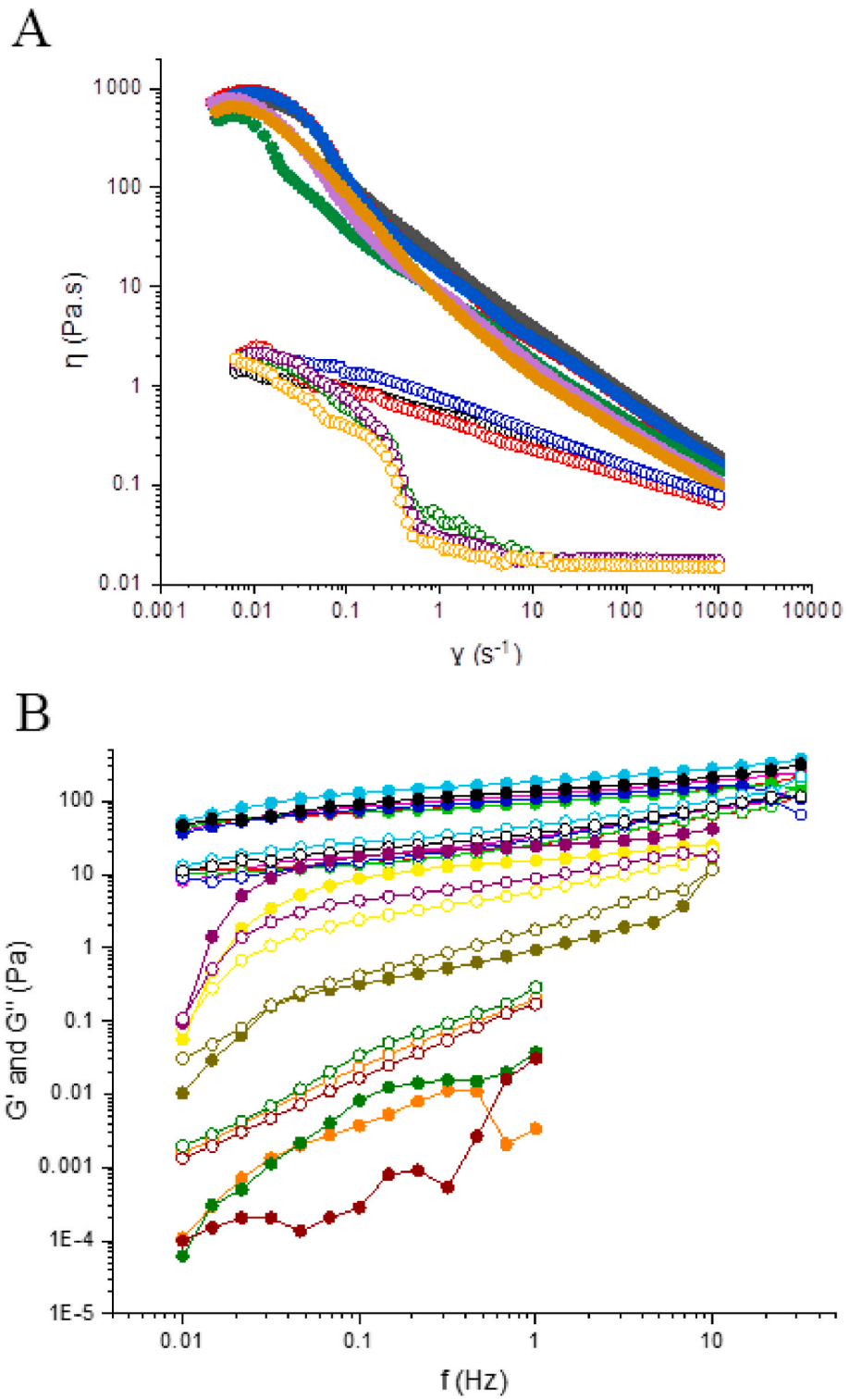

Fig. 2. Viscosity curves (● CAP-CHI 1 % control, ● CAP-CHI 1 % RCEO, ● CAP-CHI 1 % GCEO, ● CSP-CHI 1 % control, ● CSP-CHI 1 % RCEO, ● CSP-CHI 1 % GCEO, ○ CAP 5 % control, ○ CAP 5 % RCEO, ○ CAP 5 % GCEO, ○ CSP 5 % control, ○ CSP 5 % RCEO, ○ CSP 5 % GCEO) (A) and frequency sweeps (● G′ and ○ G″ CAP-CHI 1 % control, ● G′ and ○ G″ CAP-CHI 1 % RCEO, ● G′ and ○ G″ CAP-CHI 1 % GCEO, ● G′ and ○ G″ CSP-CHI 1 % control, ● G′ and ○ G″ CSP-CHI 1 % RCEO, ● G′ and ○ G″ CSP-CHI 1 % GCEO, ● G′ and ○ G″ CAP 5 % control, ● G′ and ○ G″ CAP 5 % RCEO, ● G′ and ○ G″ CAP 5 % GCEO, ● G′ and ○ G″ CSP 5 % control, ● G′ and ○ G″ CSP 5 % RCEO, ● G′ and ○ G″ CSP 5 % GCEO) (B) of 1 % pectin/chitosan and 5 % pectin solutions with green and roasted coffee EOs at 23 °C.

$_6$) of chitosan.

2.4. Rheological analyses

Rheology of pectin and pectin/chitosan solutions was performed in a Thermo Scientific Haake Rheostress1 Rheometer coupled with a Peltier/Plate TCP/P temperature control unit (Haake GmbH, Germany). Analyses were conducted with a cone/plate geometry (C35/2° Ti L) at a temperature of 23 °C. Flow behavior of pectin and pectin/chitosan solutions were performed in CR mode ($\dot{\gamma} = 0.005–1000\ s^{-1}$) and data were

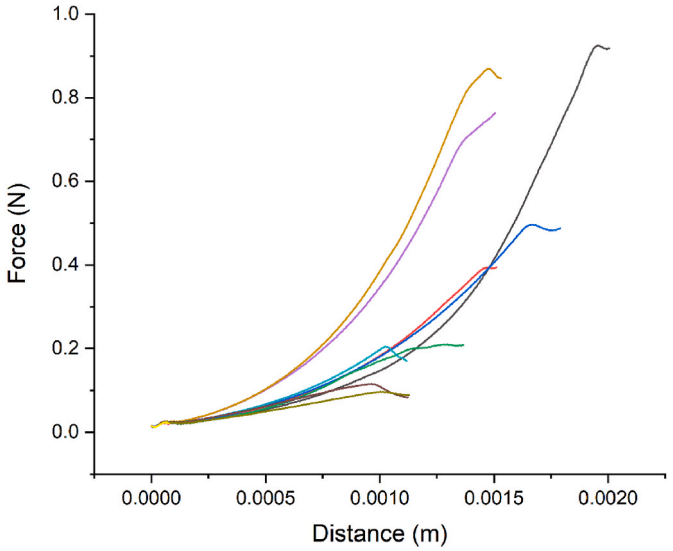

Fig. 3. Compression tests of 1 % pectin/chitosan and 5 % pectin hydrogel beads loaded with roasted and green coffee EOs. — CAP-CHI 1 % control, — CAP-CHI 1 % RCEO, — CAP-CHI 1 % GCEO, — CSP-CHI 1 % control, — CSP-CHI 1 % RCEO, — CSP-CHI 1 % GCEO, — CAP 5 % control, — CAP 5 % RCEO, — CAP 5 % GCEO, — CSP 5 % control, — CSP 5 % RCEO, — CSP 5 % GCEO).

Table 1
Strength and work values of 1 % pectin/chitosan and 5 % pectin hydrogel beads loaded with roasted and green coffee EOs. Values with different letters in each column are significantly ($p < 0.05$) different from each other.

	Strength (g)	Work (N·m)
CAP 1 % Control	21.5 ± 3.8^{a}	$9.9 \times 10^{-5} \pm 5.3 \times 10^{-5\ a}$
CAP 1 % RCEO	71.5 ± 3.7^{b}	$3.6 \times 10^{-4} \pm 4.0 \times 10^{-5\ b}$
CAP 1 % GCEO	79.2 ± 6.3^{bc}	$3.5 \times 10^{-4} \pm 2.3 \times 10^{-5\ b}$
CSP 1 % Control	88.1 ± 4.0^{c}	$4.8 \times 10^{-4} \pm 4.4 \times 10^{-5\ b}$
CSP 1 % RCEO	44.4 ± 5.7^{d}	$2.2 \times 10^{-4} \pm 3.0 \times 10^{-5\ b}$
CSP 1 % GCEO	43.6 ± 6.8^{d}	$2.3 \times 10^{-4} \pm 5.4 \times 10^{-5\ b}$
CAP 5 % Control	2.4 ± 0.1^{a}	$8.1 \times 10^{-7} \pm 9.4 \times 10^{-9\ a}$
CAP 5 % RCEO	2.4 ± 0.1^{a}	$7.9 \times 10^{-7} \pm 9.2 \times 10^{-8\ a}$
CAP 5 % GCEO	2.4 ± 0.1^{a}	$7.5 \times 10^{-7} \pm 3.5 \times 10^{-8\ a}$
CSP 5 % Control	19.8 ± 2.7^{b}	$7.1 \times 10^{-5} \pm 1.1 \times 10^{-5\ b}$
CSP 5 % RCEO	11.3 ± 1.5^{c}	$6.6 \times 10^{-5} \pm 8.9 \times 10^{-6\ bc}$
CSP 5 % GCEO	9.4 ± 1.5^{c}	$4.8 \times 10^{-5} \pm 1.1 \times 10^{-5\ c}$

fitted to the Carreau-Yasuda rheological model. Frequency sweeps (0.01–10 Hz) were performed within the linear viscoelastic region, determined by stress sweeps (0.01–1000 Pa) at 1 Hz.

2.4.1. Scanning electron microscopy (SEM)

The morphology of the beads was evaluated using a Hitachi S-4800 field emission scanning electron microscope (Hitachi High-Technologies Corporation, Spain). Samples were freeze-dried and mounted on a metal stub and coated under vacuum with gold, using a JEOL fine-coat ion sputter JFC-1100 (Izasa, Spain) in an Ar atmosphere. An acceleration voltage of 15 kV and magnifications of×50 and × 1500 were employed.

2.5. Compression tests

Uniaxial compression tests were performed to assess the strength of pectin and pectin/chitosan beads. A Stable Micro Systems TA XT Plus (Stable Micro Systems Ltd., UK) equipped with a tensile load cell of 5 kg and a 2 mm Dia stainless cylinder probe were used for the analyses. Compression resistance tests of a minimum of three samples for each composition were performed at room temperature. A velocity of 1 mm/s was used and load was applied until 80 % of the original height of the sample. The maximum force required for compression was used as an indication of the strength of the beads (Karakas, Ordu, Bozkurt, & Karadag, 2021).

2.6. Attenuated total reflection fourier transform infrared (ATR-FTIR) spectroscopy

ATR-FTIR analyses of EOs and pectin and pectin/chitosan beads were performed on a Bruker ALPHA II (Bruker, Germany). Analyses were carried out from 4000 to 500 cm^{-1}, at 4 cm^{-1} resolution, with a total of 32 scans.

2.7. X-ray diffraction (XRD)

XRD analysis was performed at 40 kV and 40 mA using a diffraction unit (PANalytic Xpert PRO, Spain). The source of radiation was Cu-Kα ($\lambda = 1.5418$ Å). The diffraction data were obtained from 2θ values from 2° to 50°, where θ is the angle of incidence of the X-ray beam on the sample.

2.8. Acid/alkali resistance

Swelling under acidic (1 M HCl) and alkali (1 M NaOH) conditions was tested for seven days to analyze the resistance of the beads under these harsh conditions. For that, the dried beads were weighed, immersed into the solutions, and had their weights measured at selected times for the calculation of swelling, as follows:

$$Swelling\ () = \frac{wt - w0}{w0} \times 100 \quad (1)$$

where *w0* and *wt* represent the weight obtained at t = 0 and t at a specific time, respectively. The first samples were analyzed after 30 min, 1 h, 2 h and 4 h of immersion and then, after 1, 2, 3 and 7 days to be able to ensure the achievement of the plateau in the swelling curve. Additionally, FTIR and X-ray analyses were conducted with the beads after swelling.

2.9. Release of coffee EOs from beads

The release of green and roasted coffee EOs was assessed by UV–Vis spectroscopy using a Multiskan Sky (Thermo Scientific, Spain). 95 % ethanol was used as a fatty food simulant. Calibration curves were constructed with different concentrations of coffee EOs (0.15625–1.25 μL/mL) at the maximum absorbance ($\lambda = 284$ nm) obtained by spectrum sweep (λ = 200–800 nm). The beads were stirred at 100 rpm in 5 mL ethanol for 24 h and 1 mL aliquots were withdrawn at different times and replaced with fresh ethanol solution. The light absorption of the samples at λ 284 nm were recorded and used to estimate the release of EOs.

2.10. DPPH radical scavenging activity

DPPH radical activity of coffee EOs (0.15625–2.5 μL EO/mL ethanol) and samples (100 mg of beads) after 24 h release in 95 % ethanol (5 mL) were measured as described by Uranga, Etxabide, Guerrero, and de la Caba (2018) with modifications. Briefly, 180 μL of the released solution was mixed with 180 μL of 75 μM DPPH solution in a 96-well plate. The

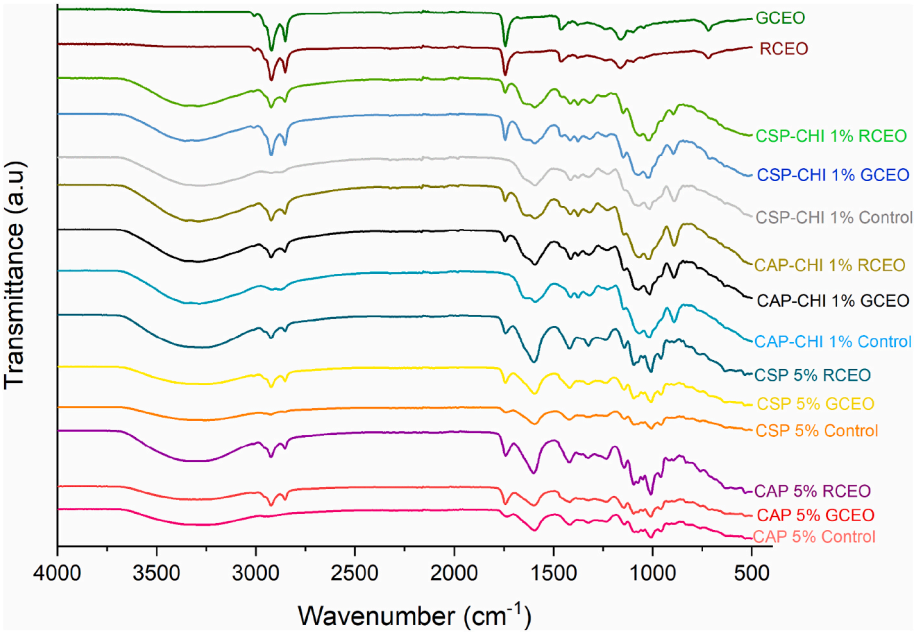

Fig. 4. FTIR spectra of green and roasted coffee EOs and hydrogel beads.

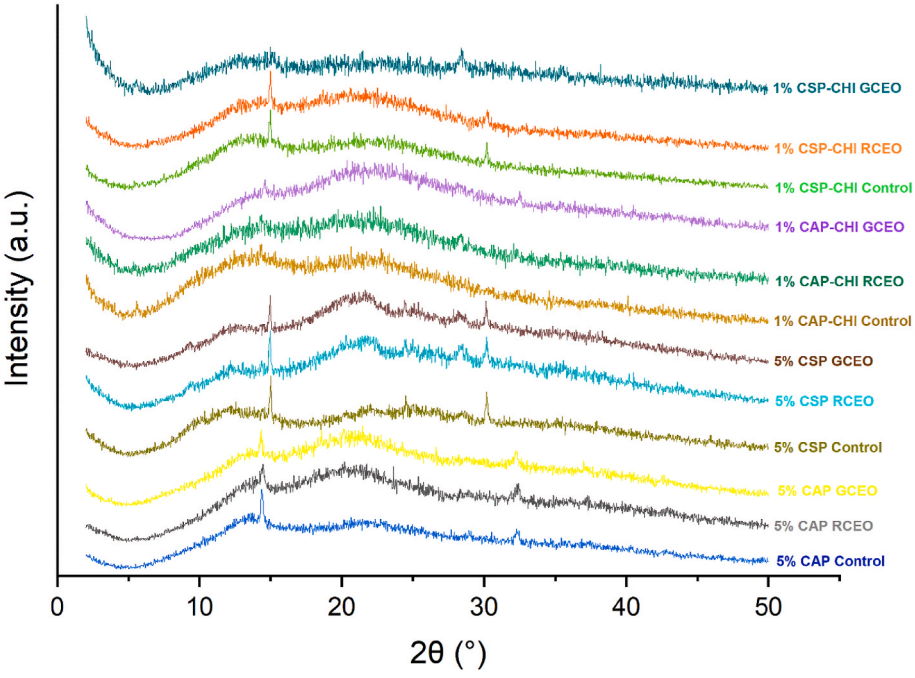

Fig. 5. XRD patterns of hydrogel beads from different formulations.

plate was kept in the dark at room temperature for 30 min. The inhibition (I) was calculated by the decrease in absorbance (A) measured at 517 nm in triplicate, as follows:

$$I\,() = \frac{A_{DPPH} - A_{sample}}{A_{DPPH}} \times 100$$

2.11. Statistical analyses

The results were expressed as mean ± SD (standard deviation). Significance (p value < 0.05 were significant) was determined by one-way analysis of variance (one-way ANOVA) followed by Tukey's multiple range test using GraphPad Prism version 5.00 (GraphPad Software Inc., USA) software.

3. Results and discussion

3.1. DA estimation of chitosan

Solid state ^{13}C NMR was used to estimate the DA of commercial chitosan, as it is an important parameter that affects solubility and polymer interactions. Signal integrals of CH_3 (δ 23.2), C═O (δ 173.8) and ring carbons (C1 δ 104.8, C2 δ 57.2, C3-5 δ 74.8, C4 δ 82.9, C6 δ 60.7) (Fig. 1) were used for the estimation of DA, which resulted in 23.7 %.

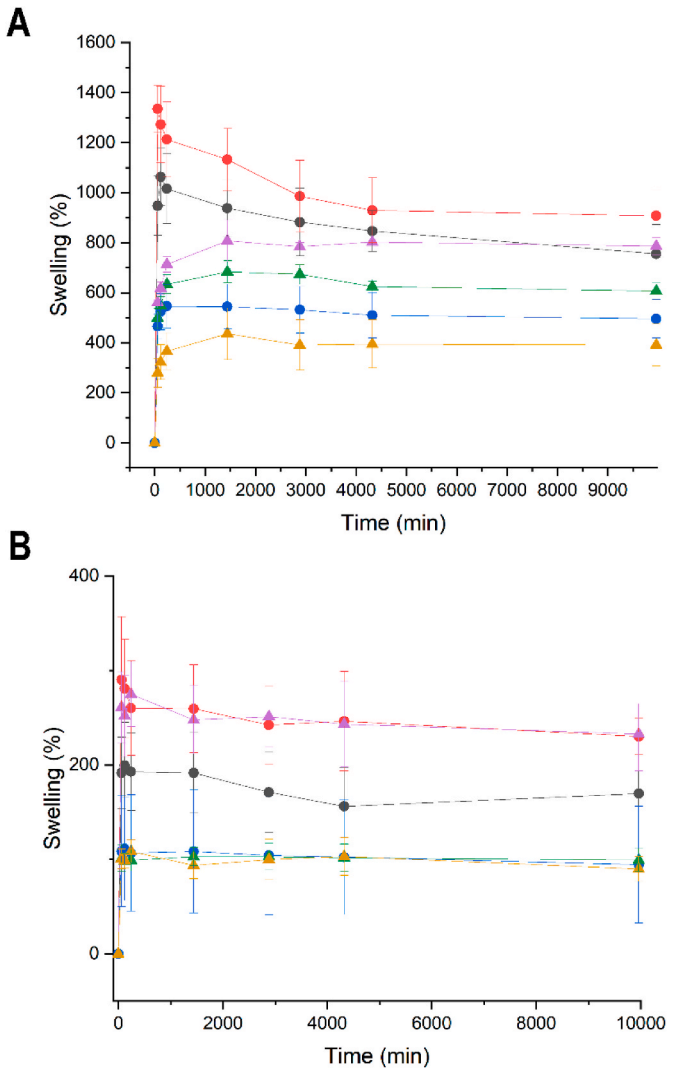

Fig. 6. Swelling of pectin/chitosan beads during 7-day treatment in 1 M HCl (A) and 1 M NaOH (B). ● CAP-CHI 1 % control, ● CAP-CHI 1 % RCEO, ● CAP-CHI 1 % GCEO, ▲ CSP-CHI 1 % control, ▲ CSP-CHI 1 % RCEO, ▲ CSP-CHI 1 % GCEO.

3.2. Rheological analyses

Rheology of solutions used in industrial processes is an important factor that can affect the manufacture of the aimed product. It can influence different steps of the process, such as mixing, pumping, storage, chemical reactions, fermentation and storage (Barnes, 2000). This is crucial when working with polymer solutions, which can produce very viscous and/or viscoelastic dispersions. In this work, viscosity curves of 1 % pectin/chitosan and 5 % pectin solutions were assessed (Fig. 2A).

The apparent viscosity values of the binary systems were higher than that of the pectin solutions over the different shear rates. Fitting to Carreau-Yasuda model (Table S1) shows that the solutions present a shear thinning behavior, with more accentuated pseudoplasticity for 1 % pectin/chitosan (n = 0–0.2) and 5 % CSP (n = 0–0.1) over 5 % CAP (n = 0.6) formulations. CAP produced the most viscous solutions and the inclusion of EOs slightly increased the zero shear rate viscosity (η_0) of CAP and CSP formulations. Similar trend was seen with the addition of tea tree EO into film forming dispersions of hydroxypropylmethylcellulose, where the apparent viscosity values slightly increased with increasing concentration of oil (Sánchez-González, Vargas, Gonzalez-Martínez, Chiralt, & Cháfer, 2009). When oil is incorporated into the system, there is some modification of the interactions of the polymers with water, leading to rheological changes (Atarés, de Jesús, Talens, & Chiralt, 2010). It is also known that in emulsified systems, oil concentration and droplet size have direct effect on viscosity, with the formation of oil droplets delaying the prompt flow of the emulsified system (Richardson, 1950).

Frequency sweeps (Fig. 2B) showed higher moduli (G′ and G″) values for pectin/chitosan blends. A gel-like behavior (G' > G") was observed for the 1 % concentration blends. For the pure pectin solutions, higher moduli values were seen for CAP solutions. A higher resistance to flow and stronger polymer network gel was observed for pectin/chitosan solutions, thus a higher shear force must be applied for these systems to produce drops for hydrogel bead formation.

3.3. Morphology and strength of the hydrogel beads

SEM micrographs of pectin/chitosan (Fig. S1A) and pectin (Fig. S1B) beads show that they present a porous structure. A smoother surface was seen for pectin/chitosan beads when compared to the pure pectin beads, evidencing the good homogeneity of the composite. A stratified morphology could be observed for the 5 % CSP beads, probably as a

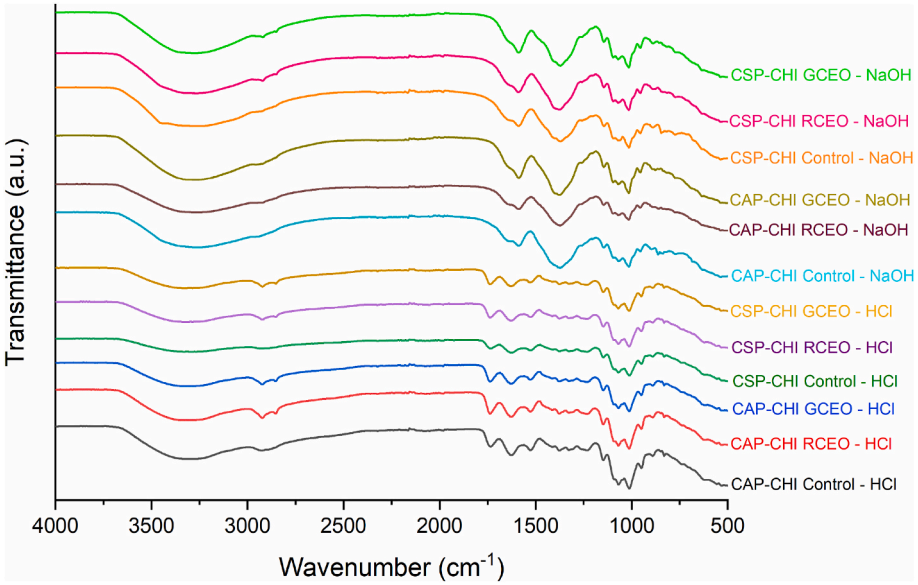

Fig. 7. FTIR spectra of hydrogel beads loaded with coffee EOs after 1 M HCl and NaOH treatments.

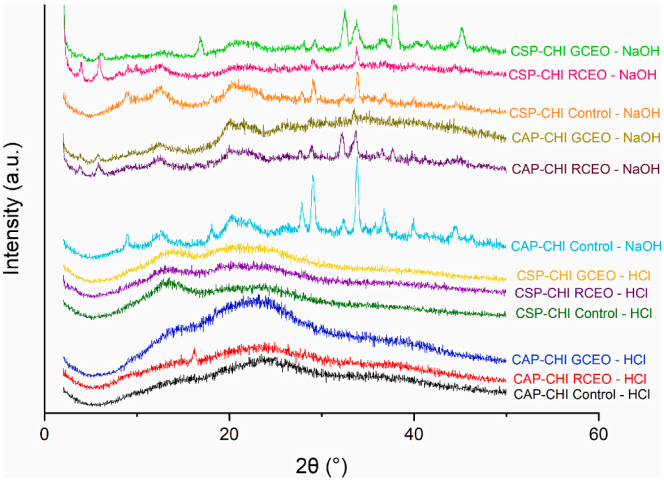

Fig. 8. XRD patterns of hydrogel beads loaded with coffee EOs after 1 M HCl and NaOH treatments.

result of a higher structural organization due to the polygalacturonate chain association promoted by electrostatic interaction with calcium ions (egg-box). Small spherical protrusions can be seen in pure pectin images (Fig. S1B), possibly as a consequence of non-encapsulated coffee EOs and/or other insoluble matter.

Compression tests were performed with the hydrogel beads (Fig. 3). The pressure applied to the surface of the hydrogel and the distance that the hydrogel is compressed can be used to evaluate the textural behavior of the different formulations (Ahearne, Yang, & Liu, 2008).

The pectin type, presence of chitosan and addition of EO influenced the mechanical properties of the beads (Table 1). Pectin/chitosan blends produced stronger beads than pectin alone. In general, the formulations using coffee pectin and chitosan were stronger (21.5–88.1 g) than those prepared using 1 % (w/v) pectin/alginate/chitosan beads loaded with ellagic acid (11.2–26.4 g) (Karakas et al., 2021). The CSP Control beads were stronger than CAP Control. However, the addition of EOs weakened CSP beads, while for CAP the beads were strengthened. Probably, the high-methoxyl content of CAP propitiated more hydrophobic interactions with the EO compounds. On the other hand, as CSP is low methyl-esterified, the EO disturbed the electrostatic interactions that helped maintaining bead integrity. Probably, the proteinaceous moiety of pectin, as well as methoxyl and acetyl groups from galacturonic acid, interact with EO compounds when the emulsion is first formed, and these interactions could prevent the amine groups of chitosan to approach carboxylate groups of pectin. For pectin alone, CAP beads were weak, since calcium is not suitable for gel formation of an HM pectin fraction. As for 1 % CSP beads, 5 % CSP beads were weakened by the addition of EOs. Oil type (green or roasted) did not produce significantly different beads regarding their mechanical properties.

3.4. Physicochemical properties of EOs and hydrogel beads

ATR-FTIR was performed in order to obtain information about chemical structure and EO incorporation (Fig. 4). The comparison of the controls from coffee pectin and pectin/chitosan beads spectra showed a shift of the carboxylate band from 1597 cm^{-1} to 1588 cm^{-1} when pectin is associated with chitosan. This indicates electrostatic interactions between the two polymers. Also, the ester band present in 5 % CSP and CAP control at 1740 cm^{-1} was not found in the 1 % pectin/chitosan controls, being displaced to 1642 cm^{-1}, suggesting that hydrophobic interactions take place between pectin and chitosan involving the methoxyl group of pectin and the N-acetyl group of chitosan. In coffee EOs, a small band at 3009 cm^{-1} was seen associated to the C–H stretching vibration of double bonds, coming from unsaturated fatty acids (Raba et al., 2015) and chlorogenic and caffeic acids (Freiberger et al., 2015). A shoulder at 2956 cm^{-1} was assigned to the stretching vibration of C–H bonds of aliphatic CH_3 groups. The bands at 2920 and 2850 cm^{-1} were respective to the stretching vibration of C–H bonds of CH_2. Stretching vibration from carbonyl from triglycerides was seen at 1743 cm^{-1}. In 1463 cm^{-1} it was possible to see the bending vibration of C–H of CH_2 and CH_3. Other smaller signals respective to alkenes were seen at 720 cm^{-1}, 1416 cm^{-1} and 1660 cm^{-1} (Raba et al., 2015). The incorporation of EOs to the beads could be confirmed by the substantial increase in the 2920 and 2850 cm^{-1} signals and the C═O band at 1743 cm^{-1}.

X-ray diffractograms (Fig. 5) showed broader peaks at 14° and 22° for the 1 % pectin/chitosan blends over the 5 % pure pectin treatment, pointing to a more amorphous structure for the pectin/chitosan composites. Sharp signals at 14.5–14.9° and 30.2–32.2° may be due to the presence of calcium chloride used for gelification or residual ammonium oxalate used for CSP extraction. It appears that the presence of green or roasted coffee oil increased the intensity of the peak at around 22°, especially for the pure pectin beads, indicating that the EO interacts with the polymer. In the study of De Souza, dos Santos, Torin, and Rosa (2020), the incorporation of Carvacrol EO in thermoplastic starch films also had an impact on the XRD pattern of films, with the highest crystallinity presented by the treatment with the highest concentration of EO. Pectin and chitosan could interact with coffee EOs, which could also act as plasticizers, increasing macromolecular mobility, which would allow the polysaccharides to form microcrystalline junctions (Bergo et al., 2008).

3.5. Acidic and basic treatments with the hydrogel beads

Acidic (1 M HCl) and basic (1 M NaOH) treatments were conducted for 7 days with the beads. Pure pectin beads were disrupted in smaller pieces within the first hour in both acid or base solution. Therefore, swelling was measured only for pectin/chitosan formulations. Overall, bead swelling was higher in HCl (Fig. 6A) than in NaOH (Fig. 6B), which can be explained by the susceptibility of polysaccharides to acid hydrolysis and consequently more potential to infiltration and bulging. This also explains the considerable weight loss present in CAP Control and RCEO after the acid treatment.

In the case of CAP GCEO, weight loss was minimized, indicating that it protected the bead against degradation. GCEO decreased the initial swelling values of the beads, while for RCEO, the swelling was increased, showing that oil type has an influence in this parameter. A comparison between alginate-polycaprolactone based films formulated with oregano, savory and cinnamon EOs showed that oil type had a great impact on the film polarity. The predominance of aldehydes on cinnamon EO eased film interaction with water, while the phenolic compounds and monoterpenes of oregano and savory EOs had less affinity with water (Salmieri & Lacroix, 2006). For coffee EOs, it is possible that the formation of multiple compounds during roasting affected the polarity and potential of the oil in forming interactions with the matrix. Regarding pectin, CAP presented greater swelling ability than CSP. This trend can be attributed to the differences in their degree of methyl-esterification. Zein-pectin microspheres swelled more when prepared with high-methoxylated citrus pectin than with low-methoxylated apple pectin (Mukhidinov et al., 2011). At first, this trend appears to contradict the theory of polyelectrolytes, where

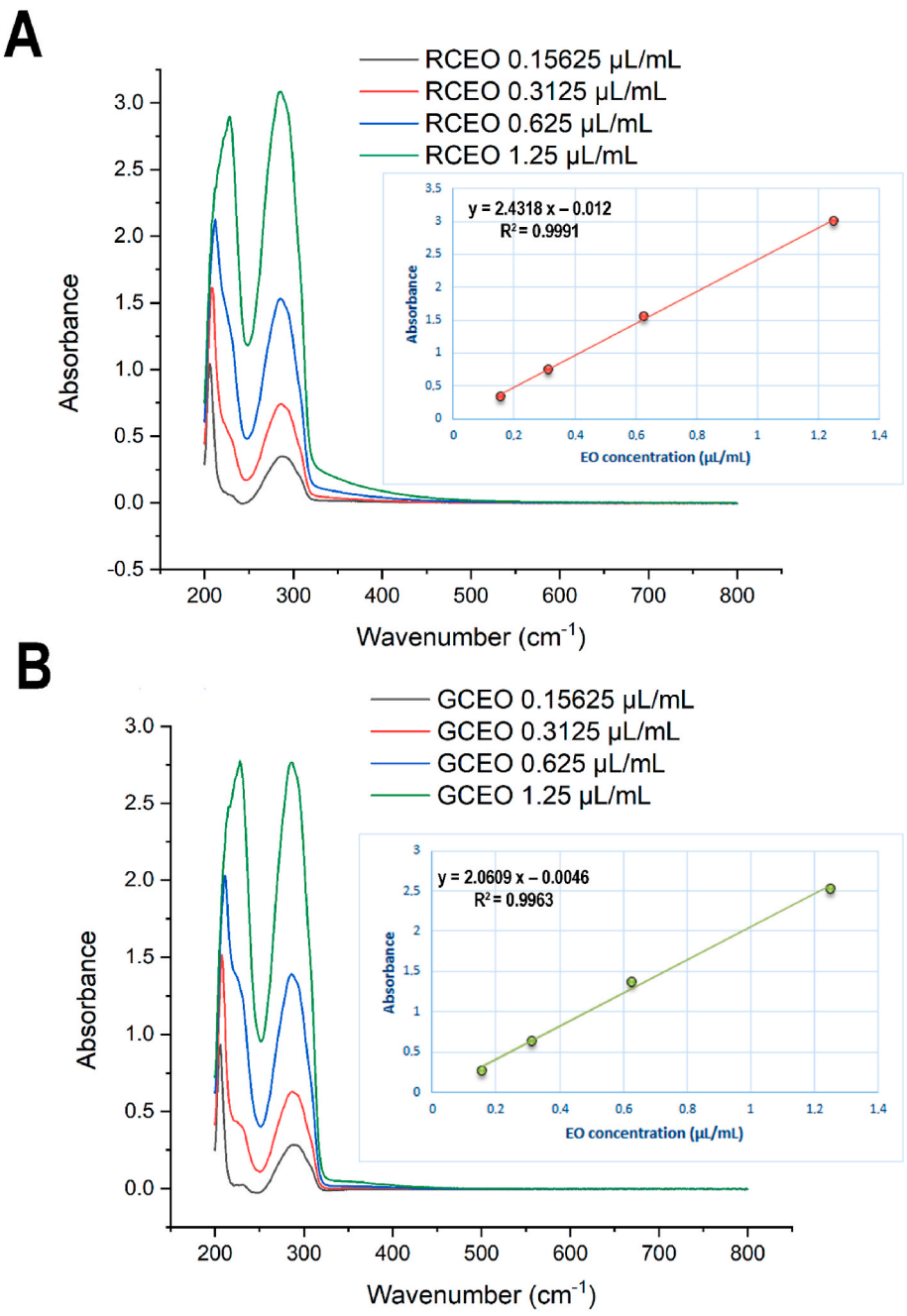

Fig. 9. UV–vis spectra of RCEO (A) and GCEO (B) at different concentrations and calibration curves at λ 284 nm.

increasing charge leads to increasing swelling. However, Zsivánovits, Marudova, and Ring (2005) have explained the phenomenon of decreased swelling for lower levels of methyl-esterification in pectins. At high charge densities, there is a condensation of counterions, which cannot participate in the Donnan type swelling effect. Also, network crosslinks contribute for lower swelling rates. In general, pectin/chitosan beads could resist both acid and base 7-day treatment and were subsequently analyzed regarding their chemical structure.

FTIR analysis was performed with the beads after acid and basic treatments (Fig. 7). It is possible to see that the spectra after the acid treatment is more similar to the original spectra (Fig. 4) than the basic one. After the NaOH treatment, C═O stretching vibration at 1743 cm^{-1} disappeared, indicating saponification of ester groups from pectins and triacylglycerols from coffee EOs. The substantial increase in the band at 1380 cm^{-1} coming from C═O symmetric stretching from carboxylate groups corroborates the occurrence of the reaction, as carboxylic acid is a product of saponification (Morales-Martínez, López-Cuellar, Chavarría-Hernández, & Rodríguez-Hernández, 2018). Some deacetylation of chitosan is seen as the band related to NH_2 bending at 1586 cm^{-1} was more intense than the band at 1644 cm^{-1} from C═O stretching of N-acetyl chitosan. It is possible to suggest that the acid modifications are more related to the diminution of polysaccharide chain length as a result of hydrolysis, not having a great impact on the FTIR spectra, while the basic ones have a severe impact in the functional groups of the compounds.

In order to obtain more information about the effect of acidic and alkali conditions on the structure of the beads, XRD analysis was performed (Fig. 8). The diffractograms after the acid treatment were similar than the previous ones, indicating few changes in crystallinity (Fig. 6). On the other hand, the XRD patterns after the basic treatment showed a

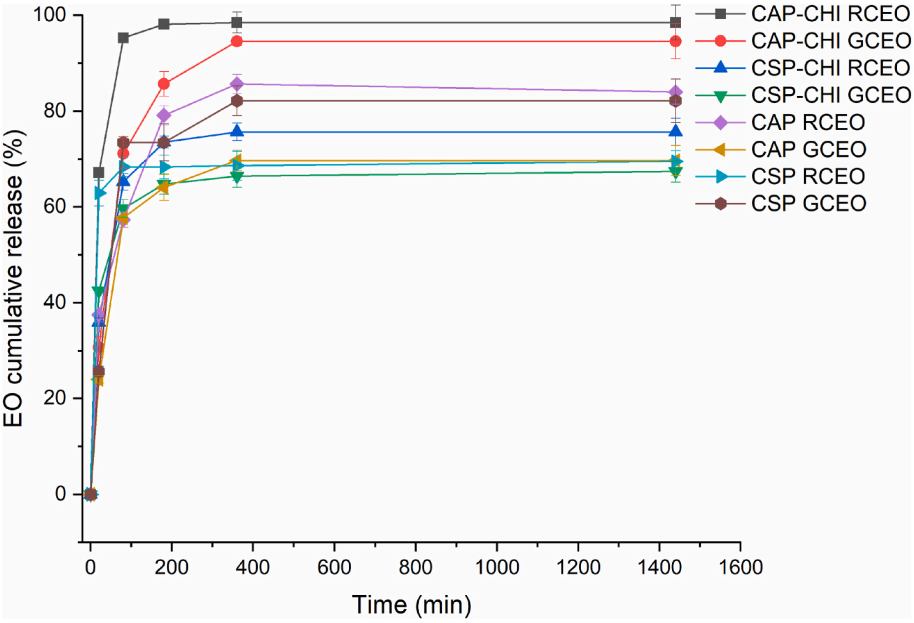

Fig. 10. Cumulative release of coffee EOs from the hydrogel beads.

much different structure, in accordance to the FTIR analysis. Changes in the length of the peaks at 14° and 22° were detected. Also, clear crystalline regions were seen, matching the crystallographic profile of trona ($Na_3H(CO_3)_2{\cdot}2H_2O$), which occurred by the reaction of atmospheric CO_2 with NaOH (Pertlik, 1986).

3.6. Release of coffee EOs from the hydrogel beads

The Commission Regulation (EU) 2016/1416 recommends vegetable oil as the primary fat simulant. In cases where technical feasibility is not achievable, migration tests can be conducted using 95 % ethanol, the fat simulant used in this study due to concerns about the interference with UV spectra caused by the unsaturation of vegetable oil, which is critical for tracking release. UV–vis analysis was performed with different coffee EOs concentrations diluted in ethanol 95 % in order to construct a calibration curve, which allowed to estimate the release of EOs from the hydrogel beads over time. Absorbances at λ 284 nm were used for curve construction after UV–vis sweeps. Sweeps and linearization of data from RCEO ($y = 2.4318\ x - 0.012$, $R^2 = 0.9991$) and GCEO ($y = 2.0609\ x - 0.0046$, $R^2 = 0.9963$) are shown in Fig. 9A and B, respectively.

Cumulative release of green and roasted coffee EOs from beads over the course of 24 h are shown in Fig. 10. It is possible to visualize that coffee EOs are readily release from the beads in ethanol, being released in a range between 31 % and 67 % of EO in the first 20 min, depending on the formulation. Total release of EOs after 24 h varied from 67 % up to 98 %, a very high value for release. In general, formulations using CAP fraction showed higher levels of release, especially when associated with chitosan. This can be explained by the degree of methyl-esterification and molecular weight of the fraction, as reported by Guan, Hua, Wang, Yuan, and Yang (2023), who reported a better encapsulation effect of soybean oil for the fraction with the highest methoxyl content and lowest molecular weight. The higher apparent viscosity values presented by the pectin/chitosan blends over the pure pectin solutions (Fig. 2) can also be related to their higher encapsulation efficiency. This tendency was also seen in the mixture of maltodextrin, gum arabic and whey protein encapsulating drumstick oil (Premi & Sharma, 2017).

The benefits of coffee consumption in living beings are generally related to its high antioxidant activity. This is mostly due to the presence of chlorogenic, ferulic, caffeic, an *n*-coumaric acids in the beans. In addition, roasting produces melanoidins (brown pigments), which act as strong antioxidants (Yashin, Yashin, Wang, & Nemzer, 2013). Some of these compounds are present in coffee EO, which possesses antioxidant activity. Fig. 11A confirms the antioxidant activity of coffee EOs as a result of their reaction with DPPH. It is possible to see that roasted coffee EO possesses higher DPPH inhibition, which can be related to the presence of volatile compounds produced during roasting. Furans, pyrazines, pyridines, pyrroles and phenolics are among the compounds that can be present in coffee oil as a result of Maillard and pyrolysis reactions during the roasting process of coffee beans (Toledo, Pezza, Pezza, & Toci, 2016).

The ethanol solution respective to each formulation after 24 h release also had their DPPH radical scavenging activity assessed (Fig. 11B). Again, the beads containing RCEO were superior as antioxidants than the ones having GCEO. The pure pectin beads presented more inhibition as a result of the higher volume of EO used in the solution, as it was based on the pectin weight. CSP beads presented the highest DPPH inhibition. As CSP Control presented inhibition activity (around 10 %), it indicates that CSP itself have antioxidant activity that enhanced the activity of the EOs.

4. Conclusions

Coffee pulp derived pectins demonstrated potential characteristics as delivery systems of EOs. The comprehensive investigation analyzed the rheological, morphological, mechanical, and physicochemical aspects of hydrogel beads, shedding light on the intricate interplay between polymer solutions and EOs. The combination with chitosan enhanced viscosity, mechanical properties and resistance to digestion of the beads. The presence of EO reinforced the beads in the case of CAP and weakened them in CSP formulations. ATR-FTIR spectroscopy and X-ray diffraction provided insights into the chemical and structural properties

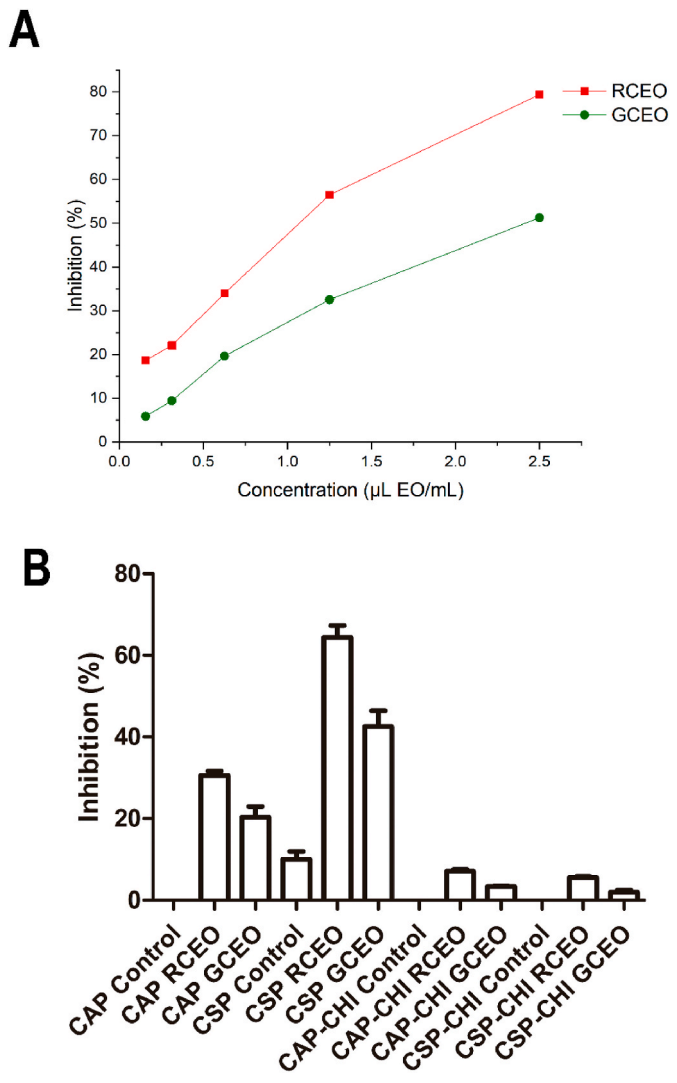

Fig. 11. DPPH radical scavenging activity of different concentrations of roasted and green coffee EOs (A) and EO loaded beads after 24 h release in 95 % ethanol (B).

of the different treatments. Release of EOs was successful and showed a superiority in encapsulation of CAP over CSP. RCEO showed to be the best oil to be used as antioxidant. The elucidation of the mechanisms governing these interactions provides a foundation for future advances in controlled release systems and food applications.

CRediT authorship contribution statement

Luis Henrique Reichembach: Writing – original draft, Investigation, Formal analysis, Data curation. **Carmen Lúcia de Oliveira Petkowicz:** Writing – review & editing, Supervision, Investigation, Funding acquisition, Formal analysis, Data curation. **Pedro Guerrero:** Writing – review & editing, Validation, Supervision, Resources, Methodology, Investigation, Conceptualization. **Koro de la Caba:** Writing – review & editing, Validation, Supervision, Resources, Project administration, Investigation, Funding acquisition, Conceptualization.

Declaration of competing interest

The authors declare that they have no known competing financial interests or personal relationships that could have appeared to influence the work reported in this paper.

Data availability

Data will be made available on request.

Acknowledgments

This work has been supported by PID 2021-124294OB-C22 project funded by MCIN/AEI/10.13039/501100011033/FEDER, UE and by the Basque Government (IT1658-22).

Appendix A. Supplementary data

Supplementary data to this article can be found online at https://doi.org/10.1016/j.foodhyd.2024.109814.

References

Ahearne, M., Yang, Y., & Liu, K.-K. (2008). Mechanical characterisation of hydrogels for tissue engineering applications. In N. Ashammakhi, R. Reis, & F. Chiellini (Eds.), *Topics in tissue engineering* (pp. 1–16).

Atarés, L., de Jesús, C., Talens, P., & Chiralt, A. (2010). Characterization of SPI-based edible films incorporated with cinnamon or ginger essential oils. *Journal of Food Engineering, 99*, 384–391.

Barnes, H. A. (2000). *A handbook of elementary rheology* (1st ed.). The University of Wales Institute of Non-Newtonian Fluid Mechanics (Chapter 19).

Bemiller, J. N. (1986). An introduction to pectins: Structure and properties. In M. L. Fishman, & J. J. Jen (Eds.), *Chemistry and function of pectins* (pp. 2–12). New York: American Chemical Society.

Bergo, P. V. A., Carvalho, R. A., Sobral, P. J. A., dos Santos, R. M. C., da Silva, F. B. R., Prison, J. M., et al. (2008). Physical properties of edible films based on cassava starch as affected by the plasticizer concentration. *Packaging Technology and Science, 21*, 85–89.

Calligaris, S., Munari, M., Arrighetti, G., & Barba, L. (2009). Insights into the physicochemical properties of coffee oil. *European Journal of Lipid Science and Technology, 111*, 1270–1277.

De Oliveira, P. M. A., de Almeida, R. H., de Oliveira, N. A., Bostyn, S., Gonçalves, C. B., & de Oliveira, A. L. (2014). Enrichment of diterpenes in green coffee oil using supercritical fluid extraction - characterization and comparison with green coffee oil from pressing. *The Journal of Supercritical Fluids, 95*, 137–145.

De Souza, A. G., dos Santos, N. M. A., Torin, R. F. S., & Rosa, D. S. (2020). Synergic antimicrobial properties of Carvacrol essential oil and montmorillonite in biodegradable starch films. *International Journal of Biological Macromolecules, 164*, 1737–1747.

FDA. (2023). Cfr - code of federal regulations - title 21. Available on https://www.accessdata.fda.gov/scripts/cdrh/cfdocs/cfcfr/cfrsearch.cfm?fr=182.20. (Accessed 26 June 2023).

Freiberger, E. B., Kaufmann, K. C., Bona, E., de Araújo, P. H. H., Sayer, C., Leimann, F. V., et al. (2015). Encapsulation of roasted coffee oil in biocompatible nanoparticles. *LWT - Food Science and Technology, 64*, 381–389.

Guan, S., Hua, X., Wang, Z., Yuan, Y., & Yang, R. (2023). Performance of ultrahigh methoxylated pectin as the delivery material in the simulated in vitro digestion. *Food Hydrocolloids, 134*, Article 108086.

Heux, L., Brugnerotto, J., Desbrières, J., Versali, M.-F., & Rinaudo, M. (2000). Solid state NMR for determination of degree of acetylation of chitin and chitosan. *Biomacromolecules, 1*, 746–751.

Ju, J., Chen, X., Xie, Y., Yu, H., Guo, Y., Cheng, Y., et al. (2019). Application of essential oil as a sustained release preparation in food packaging. *Trends in Food Science & Technology, 92*, 22–32.

Karakas, C. Y., Ordu, H. R., Bozkurt, F., & Karadag, A. (2021). Electrosprayed chitosan-coated alginate–pectin beads as potential system for colon-targeted delivery of ellagic acid. *Journal of the Science of Food and Agriculture, 102*, 965–975.

Leroux, J., Langendorff, V., Schick, G., Vaishnav, V., & Mazoyer, J. (2003). Emulsion stabilizing properties of pectin. *Food Hydrocolloids, 17*, 455–462.

Maurya, A., Prasad, J., Das, S., & Dwivedy, A. K. (2021). Essential oils and their application in food safety. *Frontiers in Sustainable Food Systems, 5*, 133.

McClements, D. J. (2017). Recent progress in hydrogel delivery systems for improving nutraceutical bioavailability. *Food Hydrocolloids, 68*, 238–245.

Mishra, R. K., Datt, M., Pal, K., & Banthia, A. K. (2008). Preparation and characterization of amidated pectin based hydrogels for drug delivery system. *Journal of Materials Science: Materials in Medicine, 19*, 2275–2280.

Morales-Martínez, Y., López-Cuellar, M.del R., Chavarría-Hernández, N., & Rodríguez-Hernández, A. I. (2018). Rheological behaviour of acetylated pectins from cactus pear fruits (*Opuntia albicarpa* and *O. matudae*). *Food Hydrocolloids, 85*, 110–119.

Mukhidinov, Z. K., Kasimova, G. F., Bobokalonov, D. T., Khalikov, D. K., Teshaev, K. I., Khalikova, M. D., et al. (2011). Pectin–zein microspheres as drug delivery systems. *Pharmaceutical Chemistry Journal, 44*, 564–567.

Ngouémazong, E. D., Christiaens, S., Shpigelman, A., Van Loey, A., & Hendrickx, M. (2015). The emulsifying and emulsion-stabilizing properties of pectin: A review. *Comprehensive Reviews in Food Science and Food Safety, 14*, 705–718.

Pertlik, F. (1986). Ein vergleich von ergebnissen routine assiger strukturbestimmungen mittels rontgen-BZW. Neutronen-einkristalldaten am beispiel der trona, Na3H[CO3] 2·2H2O. *Mitteilungen Osterreichischen Mineralogischen Gesellschaft, 131*, 7–14.

Premi, M., & Sharma, H. K. (2017). Effect of different combinations of maltodextrin, gum Arabic and whey protein concentrate on the encapsulation behavior and oxidative stability of spray dried drumstick (*Moringa oleifera*) oil. *International Journal of Biological Macromolecules, 105*, 1232–1240.

Qu, B., & Luo, Y. (2020). Chitosan-based hydrogel beads: Preparations, modifications and applications in food and agriculture sectors – a review. *Food Hydrocolloids, 152*, 437–448.

Raba, D. N., Poiana, M.-A., Borozan, A. B., Stef, M., Radu, F., & Popa, M.-V. (2015). Investigation on crude and high-temperature heated coffee oil by ATR-FTIR spectroscopy along with antioxidant and antimicrobial properties. *PLoS One, 10*, Article e0138080.

Razola-Díaz, M. del C., Guerra-Hernández, E. J., García-Villanova, B., & Verardo, V. (2021). Recent developments in extraction and encapsulation techniques of orange essential oil. *Food Chemistry, 354*, Article 129575.

Reichembach, L. H., Kaminski, G. K., Maurer, J. B. B., & Petkowicz, C. L. O. (2024). Fractionation and characterization of cell wall polysaccharides from coffee (*Coffea arabica* L.) pulp. *Carbohydrate Polymers, 327*, Article 121693.

Reichembach, L. H., & Petkowicz, C. L. O. (2020). Extraction and characterization of a pectin from coffee (*Coffea arabica* L.) pulp with gelling properties. *Carbohydrate Polymers, 245*, Article 116473.

Reichembach, L. H., & Petkowicz, C. L. O. (2021). Pectins from alternative sources and uses beyond sweets and jellies: An overview. *Food Hydrocolloids, 118*, Article 106824.

Ren, Y., Wang, C., Xu, J., & Wang, S. (2019). Cafestol and kahweol: A review on their bioactivities and pharmacological properties. *International Journal of Molecular Sciences, 20*, 4238.

Richardson, E. G. (1950). The formation and flow of emulsion. *Journal of Colloid Science, 5*, 404–414.

Salmieri, S., & Lacroix, M. (2006). Physicochemical properties of alginate/polycaprolactone-based films containing essential oils. *Journal of Agricultural and Food Chemistry, 54*, 10205–10214.

Sánchez-González, L., Vargas, M., Gonzalez-Martínez, C., Chiralt, A., & Cháfer, M. (2009). Characterization of edible films based on hydroxypropylmethylcellulose and tea tree essential oil. *Food Hydrocolloids, 23*, 2102–2109.

Toledo, P. R. A. B., Pezza, L., Pezza, H., & Toci, A. T. (2016). Relationship between the different aspects related to coffee quality and their volatile compounds. *Relationship Between the Different Aspects Related to Coffee Quality and Their Volatile Compounds, 15*, 705–719.

Tongnuanchan, P., & Benjakul, S. (2014). Essential oils: Extraction, bioactivities, and their uses for food preservation. *Journal of Food Science, 79*, 1231–1249.

Uranga, J., Etxabide, A., Guerrero, P., & de la Caba, K. (2018). Development of active fish gelatin films with anthocyanins by compression molding. *Food Hydrocolloids, 84*, 313–320.

Willats, W. G. T., Knox, J. P., & Mikkelsen, J. D. (2006). Pectin: New insights into an old polymer are starting to gel. *Trends in Food Science and Technology, 17*, 97–104.

Yashin, A., Yashin, Y., Wang, J. Y., & Nemzer, B. (2013). Antioxidant and antiradical activity of coffee. *Antioxidants, 2*, 230–245.

Zeeb, B., Saberi, A. H., Weiss, J., & McClements, J. D. (2015). Formation and characterization of filled hydrogel beads based on calcium alginate: Factors influencing nanoemulsion retention and release. *Food Hydrocolloids, 50*, 27–36.

Zsivánovits, G., Marudova, M., & Ring, S. (2005). Influence of mechanical properties of pectin films on charge density and charge density distribution in pectin macromolecule. *Colloid and Polymer Science, 284*, 301–308.